2023 31st Mediterranean Conference on Control and Automation (MED)
June 26 - 29, 2023. Limassol, Cyprus

2023 31st Mediterranean Conference on Control and Automation (MED) | 979-8-3503-1543-1/23/$31.00 ©2023 IEEE | DOI: 10.1109/MED59994.2023.10185681

Dynamic Centrality in Metapopulation Networks: Incorporating Dynamics and Network Structure

Atefe Darabi[1] and Milad Siami[1]

***Abstract*— In epidemic networks, walk-based centrality indices are often used to identify the nodes that are significantly contributing to the spread of disease. While the network topology can provide a good insight into how the disease might propagate throughout the network, epidemic-related factors can change the ranking results as well. This paper presents a *dynamics-based* node centrality that incorporates epidemic characteristics, internal time delays, and network structure at the same time. This centrality allows for dynamic identification of the nodes that are more sensitive to external shocks, which in turn can help prevent performance degradation in the network. It is shown that some of the prominent walk-based centralities, such as local and eigenvector centralities, are in fact correlated with dynamics-based centrality for certain epidemic parameters.**

I. Introduction

The emergence of contagious diseases has directed scholars' attention toward networked models to capture the epidemic behavior at the community level [1]. In many of these studies the effect of internal time delays, resulting from the latent period of a disease, has been modeled by including an extra compartment called *exposed*, e.g., Susceptible-Exposed-Infected-Removed (SEIR) model [2], [3]. However, it is shown that the behavior of models with an exposed compartment is not necessarily identical to models that directly include the effect of internal time delays [4], [5]. In other words, epidemic models defined based on ordinary differential equations (with or without considering the exposed group) fail to show the successive waves of epidemic, common in several epidemic diseases [6].

From the network robustness point of view, the performance of noisy linear consensus networks has been investigated in [7], where a performance measure based on the $\mathcal{H}_2$ norm of the system is developed. The proposed performance measure is then adopted to analyze the robustness of delayed networks with linear SIS dynamics against exogenous noises [8]. This is a metric defined based on transportation network topology, epidemic characteristics, internal time delays, and noise variance, which provides an insight into the impact of each of those components.

This material is based upon work supported by the U.S. Department of Homeland Security under Grant Award Number 22STESE00001-01-00. The views and conclusions contained in this document are those of the authors and should not be interpreted as necessarily representing the official policies, either expressed or implied, of the U.S. Department of Homeland Security. This research was supported in part by grants NSF 2208182, ONR N00014-21-1-2431, and NSF 2121121.

[1]Department of Electrical & Computer Engineering, Northeastern University, Boston, MA 02115 USA (e-mails: {darabi.a, m.siami}@northeastern.edu).

Regarding the identification of central individuals in a network, some studies have investigated the correlation between various centralities that are defined based on network structure (adjacency matrix) [9]. For instance, it is shown that parameterized centralities like Katz centrality and subgraph centrality can be "tuned" to interpolate between walk-based centralities such as degree and eigenvector centrality [10]. Various research studies have employed these walk-based centralities to develop epidemic control approaches [11]–[13]. This study is mainly focused on the notion of centrality in noisy delayed epidemic networks with the following contributions.

i. We first present the SIS dynamics of epidemic networks affected by time delay. The objective is to investigate the role of network properties and time delays in emerging successive epidemic waves under linear SIS dynamics (Section II).
ii. We then evaluate the robustness of such delayed systems against external shocks affecting the epidemic network. A metric of network performance is employed to analyze performance sensitivity against noises and delays (Section III).
iii. A specific dynamics-based node centrality index is defined to evaluate the role of each node in epidemic progress when an exogenous noise is present. Unlike many widely used centralities, e.g., degree or eigenvector centrality, this dynamics-based centrality measure does not merely depend on network structure; it is affected by epidemiological properties of the disease, such as epidemic rates and internal time delays. This unique characteristic makes this dynamics-based centrality index an ideal candidate for identifying the key nodes in epidemic networks. The relationship between dynamics-based centrality and some well-known centralities is also investigated (Section IV).

The simulation results for a network of the United States' busiest airports are presented in Section V.

II. Delayed SIS model for epidemic networks

A. Background and definitions

We denote an undirected and weighted (with or without loops) graph by $\mathcal{G} = (\mathcal{V}, \mathcal{E}, \mathbf{w})$. $\mathcal{G}$ is defined by $\mathcal{V}$, a set of $n \in \mathbb{N}$ nodes, $\mathcal{E} \subseteq \{(i,j)|i,j \in \mathcal{V}\}$, a set of $m \in \mathbb{N}$ weighted edges, and $\mathbf{w}$, the vector of weights $w_e \in \mathbb{R}_+$ for all $e = (i,j) \in \mathcal{E}$. The adjacency matrix of the corresponding

network is then defined by $A = [a_{ij}] \in \mathbb{R}^{n\times n}$, where

$$a_{ij} = \begin{cases} w_e & \text{if } e = \{i,j\} \in \mathcal{E} \\ 0 & \text{otherwise}. \end{cases} \tag{1}$$

We consider an epidemic network comprising n subpopulations/nodes in $\mathcal{V}$, where each subpopulation can be in one of two states, susceptible to the infectious disease or infected by the disease. The map of connection between the subpopulations is given by set $\mathcal{E}$. The interpopulation connection strength, i.e., traffic flow, is denoted by $0 < a_{ij} = w_e \leq 1$ for all $e \in \mathcal{E}$. The disease progress in each subpopulation of the network depends on its intrapopulation and interpopulation connections, as well as epidemic rates of the disease. While the effect of interpopulation connections is reflected through the off-diagonal elements of the adjacency matrix, its diagonal elements indicate the intensity of intrapopulation connections. We project the final effect of local (intrapopulation) social distancing between members of subpopulation i on a_{ii}, where $a_{ii} \to 0$ belongs to a subpopulation which follows the local social distancing and as $a_{ii} \to 1$, the local social distancing rules become less strict.

B. Deterministic SIS metapopulation model with time delay

This subsection briefly introduces the deterministic SIS dynamics of a delayed epidemic network with underlying graph $\mathcal{G}$. The multi-delayed SIS dynamics of epidemic networks has been thoroughly investigated in [14], where local and global time delays are considered. Note that in this study, it is assumed that local and global time delays are identical.

We employ mean-field approximation to derive the delayed SIS dynamics, where we assume that every subpopulation/node has a constant population size and is experiencing a time delay τ.

Let $p_i(t) \in [0,1]$ be the marginal probability of subpopulation i being infected at time t such that $p_i(t) = 1$ if the entire population of i is infected and $p_i(t) = 0$ if it is completely susceptible. Therefore, $p_i(t)$ can be interpreted as the fraction of infected individuals in subpopulation i at time t. The approximated deterministic dynamics of node i can then be described by

$$\begin{cases} \dot{p}_i(t) = \beta(1-p_i(t)) \sum_{j=1}^{n} a_{ij} p_j(t-\tau) - \delta p_i(t-\tau); \quad t \geq \tau \\ p_i(t) = \phi_i(t); \quad t \leq \tau, \end{cases} \tag{2}$$

where $\beta \in \mathbb{R}_+$ is the infection rate and $\delta \in \mathbb{R}_+$ is the recovery rate. $\phi_i(t)$ is the initial history function of infection for node i.

Using (2), the n-intertwined SIS model of network can now be expressed below

$$\begin{cases} \dot{\mathbf{p}}(t) = \mathcal{A}\mathbf{p}(t-\tau) - \beta P(t) A \mathbf{p}(t-\tau); \quad t \geq \tau \\ \mathbf{p}(t) = \boldsymbol{\phi}(t); \quad t \leq \tau, \end{cases} \tag{3}$$

where $\mathbf{p}(t) = [p_1(t), \ldots, p_n(t)]^\top$, $\boldsymbol{\phi}(t) = [\phi_1, \ldots, \phi_n]^\top$, $P(t) = \operatorname{diag}(\mathbf{p}(t))$, and $\mathcal{A} = \beta A - \delta I_n$. The sorted eigenvalues of $\mathcal{A}$ and A are denoted by $\lambda_1 \leq \lambda_2 \leq \ldots \leq \lambda_n$ and $u_1 \leq u_2 \leq \ldots \leq u_n$, respectively. The non-negative adjacency matrix of network can be decomposed by $A = VUV^\top$, where $V = [\mathbf{v}_1, \mathbf{v}_2, \cdots, \mathbf{v}_n]$ is orthogonal and $U = \operatorname{diag}([u_1, u_2, \cdots, u_n])$. Note that the eigenvalues of adjacency matrix A are connected to those of $\mathcal{A}$ by $u_i = \frac{\lambda_i + \delta}{\beta}$ for all $i \in \mathcal{V}$. Linearization of equation (3) around its disease-free equilibrium, $\mathbf{p}^*(t) = 0$, provides the following linear SIS dynamics [15]

$$\begin{cases} \dot{\mathbf{p}}(t) = \mathcal{A}\mathbf{p}(t-\tau); \quad t \geq \tau \\ \mathbf{p}(t) = \boldsymbol{\phi}(t); \quad t \leq \tau. \end{cases} \tag{4}$$

The stability of an epidemic network that follows the linear dynamics (4) is previously studied in [14], [16]. It is shown that for a network with dynamics (4) and $\mathcal{R}_{0M} < 1$, if $0 < \tau < -\frac{\pi}{2\lambda_1}$, then the asymptotic stability is guaranteed.

The basic reproduction number of an epidemic network, $\mathcal{R}_{0M}$, is a metric that provides the expected number of neighbors an infected subpopulation will infect. For a metapopulation with dynamics (4), the network reproduction number is defined below

$$\mathcal{R}_{0M} := 1 + \frac{\lambda_n}{\delta}. \tag{5}$$

III. Performance analysis in the presence of small shocks

In this section, the performance deterioration of linear network (4) subject to small shocks is investigated. The effect of shock on the infection dynamics of subpopulation i is modeled by an additive white noise such that $\xi_i(t) \sim \mathcal{N}(0, \sigma_i^2)$[1], and it is assumed that the input noise for each subpopulation is independent of the others [17], [18], i.e., $\boldsymbol{\xi}(t) = [\xi_1(t), \xi_2(t), \ldots, \xi_n(t)]^\top$, where $\boldsymbol{\xi}(t) \sim \mathcal{N}\left(\mathbf{0}_n, \operatorname{diag}\left([\sigma_1^2, \sigma_2^2, \ldots, \sigma_n^2]\right)\right)$. An $\mathcal{H}_2$-based performance measure is adopted from [7] to find an explicit representation for the network performance loss. This $\mathcal{H}_2$ norm-based measure quantifies fluctuations in the average number of infected people based on the steady-state variance of nodal state fluctuations.

Assume that the exogenous noise input described earlier is affecting the dynamics of network (4) as shown below

$$\begin{cases} \dot{\mathbf{p}}(t) = \mathcal{A}\mathbf{p}(t-\tau) + \boldsymbol{\xi}(t); \quad t \geq \tau \\ \mathbf{p}(t) = \boldsymbol{\phi}(t); \quad t \leq \tau. \end{cases} \tag{6}$$

According to [19], the performance measure ρ_{ss} of a stable system (6) with transfer function $G(j\omega)$ can be found by the frequency domain definition of its $\mathcal{H}_2$ norm as follows

$$\rho_{\text{ss}} = \frac{1}{2\pi} \operatorname{Tr}\left[\int_{-\infty}^{+\infty} G^{\text{H}}(j\omega) G(j\omega) d\omega\right], \tag{7}$$

where $G^{\text{H}}(j\omega)$ corresponds to the complex conjugate transpose of $G(j\omega)$. ρ_{ss} measures the performance loss of network; therefore, smaller values of ρ_{ss} result in a better performance.

[1]The notation $\mathcal{N}(0, \sigma_i^2)$ represents a normal distribution with mean 0 and variance σ_i^2.

For the network system with dynamics (6), let $\hat{\xi}_i \coloneqq \frac{\xi_i}{\sigma_i}$ for all $i \in \mathcal{V}$. We then have $\boldsymbol{\xi} = B\hat{\boldsymbol{\xi}}$, where $\hat{\boldsymbol{\xi}} = [\hat{\xi}_1, \hat{\xi}_2, \ldots, \hat{\xi}_n]$ and $B = \operatorname{diag}([\sigma_1, \sigma_2, \ldots, \sigma_n])$. Note that $\hat{\boldsymbol{\xi}}$ is a vector of unit variance and identically distributed Gaussian processes. We next define $G(j\omega)$ as the transfer function from $\hat{\boldsymbol{\xi}}(t)$ to $\mathbf{p}(t)$ and present the closed-form solution of (7) by

$$\rho_{\text{ss}} = \sum_{i=1}^{n} -\frac{\Phi_i}{2\lambda_i} \frac{\cos(\lambda_i \tau)}{1 + \sin(\lambda_i \tau)}, \tag{8}$$

in which Φ_i is the i^{th} diagonal element of the matrix $Q^\top B B^\top Q$, where $Q = [\mathbf{q}_1, \ldots, \mathbf{q}_n] \in \mathbb{R}^{n \times n}$ is the orthonormal matrix of eigenvectors of $\mathcal{A}$.

The network performance measure (8) can be expressed by the following compact matrix operator form

$$\rho_{\text{ss}} = -\frac{1}{2} \operatorname{Tr}\left[B B^\top \mathcal{A}^{-1} \cos(\tau\mathcal{A}) \left(I_n + \sin(\tau\mathcal{A})\right)^{-1} \right]. \tag{9}$$

IV. DYNAMICS-BASED CENTRALITY INDEX

In what follows, we define a node centrality index based on network's sensitivity to small shocks, and provide its closed form as a function of transportation network topology (adjacency matrix), epidemic rates (recovery and infection rates), and internal time delays.

Consider system (6) with an additive Gaussian white noise, $\xi_i(t) \sim \mathcal{N}(0, \sigma_i^2)$ for all $i \in \mathcal{V}$. We define the dynamics-based centrality of subpopulation i by the rate of network performance measure (9) with respect to the noise variance as shown below

$$\begin{aligned} \eta_i \coloneqq & \frac{\partial \rho_{\text{ss}}}{\partial \sigma_i^2} \\ = & -\frac{1}{2} \left[\mathcal{A}^{-1} \cos(\tau\mathcal{A}) \left(I_n + \sin(\tau\mathcal{A})\right)^{-1} \right]_{ii}, \end{aligned} \tag{10}$$

for all $i \in \mathcal{V}$. Note that $\mathcal{A} = \beta A - \delta I_n$ and operator $[.]_{ii}$ returns the i^{th} diagonal element of its matrix argument.

Network performance measure ρ_{ss} can now be retrieved using (10) as shown below

$$\rho_{\text{ss}} = \sum_{i \in \mathcal{V}} \eta_i \sigma_i^2. \tag{11}$$

Moreover, the series expansion of dynamics-based centrality η_i can be obtained by

$$\begin{aligned} \eta_i = & c_0(\delta\tau) + \frac{\beta}{\delta} c_1(\delta\tau)[A]_{ii} + \frac{\beta^2}{\delta^2} c_2(\delta\tau)[A^2]_{ii} + \cdots \\ = & \sum_{k=0}^{\infty} \frac{\beta^k}{\delta^k} c_k(\delta\tau)[A^k]_{ii} \end{aligned} \tag{12}$$

where

$$c_0(\delta\tau) = \frac{\cos(\delta\tau)}{2\delta(1 - \sin(\delta\tau))}, \; c_1(\delta\tau) = \frac{\cos(\delta\tau) - \delta\tau}{2\delta(1 - \sin(\delta\tau))},$$

and

$$\begin{aligned} c_2(\delta\tau) = & \frac{2(\cos(\delta\tau) - \delta\tau)(1 - \sin(\delta\tau))^2}{4\delta(1 - \sin(\delta\tau))^3} \\ & + \frac{\delta^2\tau^2 \cos(\delta\tau)(\cos(\delta\tau) - \sin(\delta\tau) + \sin^2(\delta\tau))}{4\delta(1 - \sin(\delta\tau))^3}. \end{aligned} \tag{13}$$

The dynamics-based centrality η_i can then be interpreted as a walk-based index that penalizes a walk of length k by $\frac{\beta^k}{\delta^k} c_k(\delta\tau)$. This notion is particularly close to the *resolvent subgraph centrality* defined in the next subsection.

A. Correlation with resolvent centrality

The resolvent centrality (a.k.a. resolvent subgraph centrality) of undirected network (6) with weighted adjacency matrix A is defined by

$$\begin{aligned} RC_i(\alpha) = & \left[(I_n - \alpha A)^{-1} \right]_{ii} \\ = & 1 + \alpha[A]_{ii} + \alpha^2[A^2]_{ii} + \cdots + \alpha^k[A^k]_{ii} + \cdots \\ = & \sum_{k=0}^{\infty} \alpha^k [A^k]_{ii}, \end{aligned} \tag{14}$$

where $[A]_{ii}$ indicates the weight of self-loop for node i. $[A^k]_{ii}$ computes the sum of weighted closed walks of length k starting from i. α is bounded above by the inverse of A's largest eigenvalue to ensure that $I_n - \alpha A$ is invertible and that its power series converges to its inverse. Note that the largest eigenvalue of A is denoted by u_n; therefore, $0 < \alpha < \frac{1}{u_n}$. Resolvent centrality of node i presents the sum of weighted closed walks of length k for $k = 0, 1, 2, \cdots$, where weighted closed walks of length k are penalized by α^k. The following theorem presents a correlation between dynamics-based and resolvent centralities.

Theorem 1: For undirected epidemic network (6) over a weighted (or unweighted) graph $\mathcal{G}$ with adjacency matrix $A = [a_{ij}] \in \mathbb{R}^{n \times n}$, infection rate β, and recovery rate δ, as $\tau \to 0$, node rankings obtained by dynamics-based centrality η_i converge to that provided by resolvent centrality RC_i, where $\alpha = \frac{\beta}{\delta}$.

B. Correlation with local centralities

We define the following local centrality for epidemic network (6) with adjacency matrix $A = [a_{ij}]$

$$o_i \coloneqq [A]_{ii} = a_{ii}, \tag{15}$$

which is dependent on local social distancing status (self-loops) in the network. We also introduce another local centrality for epidemic network (6) as follows

$$l_i \coloneqq [A^2]_{ii} = \sum_{j=1}^{n} a_{ij}^2, \tag{16}$$

which returns the sum of weighted closed walks with length 2 starting from node i. Note that for an unweighted undirected network with no self-loops, l_i turns the degree centrality of node i, which is a special version of local centrality. We denote the output of rankings obtained using centrality measures η_i, o_i, and l_i by $\mathcal{I}_e$, $\mathcal{I}_o$, and $\mathcal{I}_l$, respectively. In other words, $\mathcal{I}_e$, $\mathcal{I}_o$, and $\mathcal{I}_l$ present the set of nodes ranked in

a descending order based on the value of their corresponding centrality index. In what follows, the reverse order of a set $\mathcal{I}$ is denoted by $\mathrm{R}(\mathcal{I})$. In the following theorem, we propose a correlation between local centralities and dynamics-based centrality when the ratio of infection rate to recovery rate is close to zero, i.e., the disease is not highly contagious.

Theorem 2: For epidemic network (6) over a weighted undirected graph $\mathcal{G}$ with adjacency matrix $A = [a_{ij}] \in \mathbb{R}^{n\times n}$, infection rate β, recovery rate δ, and time delay $0 < \tau < \frac{-\pi}{2\lambda_1}$, if $\frac{\beta}{\delta} \to 0^+$, the following statements hold.

(i) When all subpopulations follow local social distancing (graph $\mathcal{G}$ with adjacency matrix A is loop-less), i.e., $a_{ii} = 0$ for all $i \in \mathcal{V}$, then

$$\mathcal{I}_e = \mathcal{I}_l. \tag{17}$$

(ii) When some subpopulations follow local social distancing (graph $\mathcal{G}$ with adjacency matrix A contains loops), i.e., $a_{ii} \neq 0$ for some $i \in \mathcal{V}$, then

$$\mathcal{I}_e = \begin{cases} \mathcal{I}_o & \text{if} \quad 0 < \delta\tau < z_1 \\ \mathcal{I}_l & \text{if} \quad \delta\tau = z_1 \\ \mathrm{R}(\mathcal{I}_o) & \text{if} \quad z_1 < \delta\tau < \frac{\pi}{2}, \end{cases} \tag{18}$$

where $z_1 \approx 0.739$ is the numerical solution to $c_1(z_1) = 0$ such that $z_1 < \frac{\pi}{2}$ (see (12)).

It can be inferred that the local centralities l_i and o_i can provide an appropriate node ranking for network (6) only when less contagious diseases are spreading. However, since these local node centralities provide a fixed ranking list regardless of the disease status, one can not rely on those indices to dynamically identify the central nodes as the disease progresses.

C. Correlation with eigenvector centrality

The eigenvector centrality for epidemic network (6) with adjacency matrix $A = [a_{ij}]$ is obtained by

$$ev_i \coloneqq \mathbf{e}_i^\top \mathbf{v}_n = \mathbf{v}_n(i), \tag{19}$$

where $\mathbf{e}_i$ is the i^{th} standard basis vector and $\mathbf{v}_n$ is the dominant eigenvector of matrix A associated with its largest eigenvalue u_n. Since network (6) is undirected, we can decompose its non-negative adjacency matrix by $A = VUV^\top$, where $V = [\mathbf{v}_1, \mathbf{v}_2, \cdots, \mathbf{v}_n]$ is orthogonal and $U = \mathrm{diag}([u_1, u_2, \cdots, u_n])$. Note that based on Perron-Frobenius theorem, a connected graph with non-negative adjacency matrix A has a non-negative real eigenvalue, which has the maximum absolute value among all eigenvalues, that is $|u_1| \leq \cdots \leq |u_{n-1}| < u_n$. The eigenvector associated with u_n can be chosen to have non-negative real entries, i.e., $\mathbf{v}_n > 0$.

We denote the output of node ranking based on eigenvector centrality ev_i by $\mathcal{I}_{ev}$, and present the following theorem to connect the dynamics-based centrality and eigenvector centrality for certain ranges of epidemic rates.

Theorem 3: For epidemic network (6) over a weighted undirected graph $\mathcal{G}$ with adjacency matrix $A = [a_{ij}] \in \mathbb{R}^{n\times n}$, infection rate β, recovery rate δ, and time delay $\tau \to 0$, if $\frac{\beta}{\delta} \to \frac{1}{u_n}^-$, then the ranking provided by dynamics-based centrality, $\mathcal{I}_e$, converges to that obtained by eigenvector centrality, $\mathcal{I}_{ev}$.

D. Interlacing nodes in dynamics-based centrality

As shown in the previous subsections, rankings obtained by dynamics-based centrality are subject to change as time delay or epidemic rates change, which results in having interlacing nodes (nodes with variable ranks) as the disease progresses. This phenomenon is consistent with what happens as an epidemic disease progresses in a cluster of connected communities; as the disease circulates in the network, different communities become more critical. This subject is further studied in this subsection.

Definition 1: Two nodes i and j of graph $\mathcal{G}$ are cospectral if for every integer $k \geq 0$, we have $[A^k]_{ii} = [A^k]_{jj}$.[2]

Definition 2: Two non-cospectral nodes i and j of graph $\mathcal{G}$ interlace at $\frac{\beta}{\delta}$ if $\eta_i\Big|_{\frac{\beta}{\delta}} = \eta_j\Big|_{\frac{\beta}{\delta}}$; $\frac{\beta}{\delta}$ is an interlacing value.

We should note that two cospectral nodes also have the same degree, eigenvector, and dynamics-based centrality measures. The following theorem provides an upper bound on the number of interlacing values for every pair of nodes in the non-delayed version of network (6) when dynamics-based centrality is incorporated.

Theorem 4: Consider the epidemic network (6) over graph $\mathcal{G}$. For any two non-cospectral nodes $i, j \in \mathcal{V}$, there can be at most $n-1$ interlacing values for dynamics-based centrality when $\tau = 0$.

V. Case Study

Air transportation plays an important role in introducing a new disease to a metapopulation and spreading it within its subpopulations. In this regard, we have implemented our simulations on a group of United States' busiest airports as a representative of an epidemic network; the airports are the network nodes, which connect to other nodes by air traffic. This network includes $|\mathcal{V}| = n = 15$ airports and $|\mathcal{E}| = m = 104$ weighted connections between them, see Fig. 1. The weight of connections is determined based on the available data in [21], which provides the total number of flights between every two airports during a certain year. The interconnection between every pair of nodes is ranked based on air traffic volume between them, which is specified by the color of links. The airports are ranked based on their dynamics-based centrality index, η_i, which is indicated by the size of circles located in the position of each airport.

Fig. 2 shows the average infection size of network, $\bar{p}(t) = \frac{1}{n}\sum_{i\in\mathcal{V}} p_i(t)$, with nonlinear dynamics (3) and different time delays when 50 percent of the metapopulation is initially infectious and $\mathcal{R}_{0M} = 2.3$. For the network with no delay, $\tau = 0$ days, or comparatively small delays, there would be no fluctuations in the epidemic dynamics but as the delay increases, epidemic pulses begin to appear. Experiencing

[2]Equivalently, two vertices i and j in a graph $\mathcal{G}$ are cospectral if the node-removed subgraphs $\mathcal{G}\backslash\{i\}$ and $\mathcal{G}\backslash\{j\}$ have the same characteristic polynomial (cf. [10], [20]).

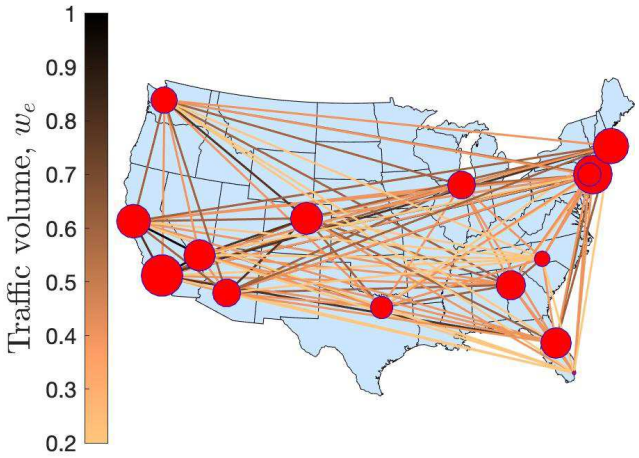

Fig. 1. (a) Network of United States' busiest airports with 15 subpopulations and their normal air traffic volume. All the subpopulations are experiencing 11 days of time delay. The hubs are ranked based on their dynamics-based centrality index, η_i, which is reflected through the size of their indicating circle. The interconnections are ranked by their corresponding traffic volume which is specified by the color of edges. The basic reproduction number of this network is $\mathcal{R}_{0M} = 0.892$.

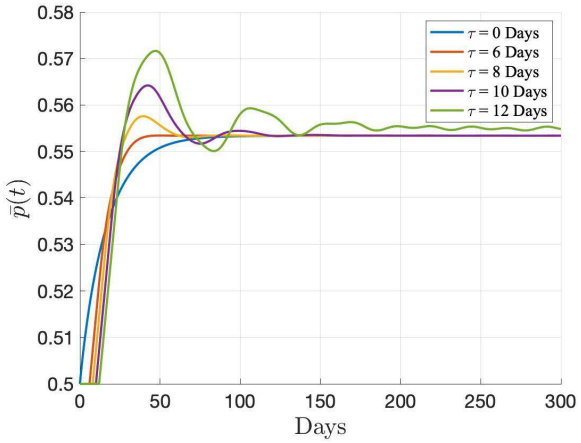

Fig. 2. Average infection size of network (3) with different time delays. 50 percent of the metapopulation is initially infectious and $\mathcal{R}_{0M} = 2.3$.

TABLE I

TOP 4 AIRPORT RANKINGS BY DYNAMICS-BASED CENTRALITY FOR DIFFERENT VALUES OF $\mathcal{R}_{0M}$ WHEN $\tau \to 0$.

Rank	$0 < \mathcal{R}_{0M} \leq 0.06$	$\mathcal{R}_{0M} = 0.5$	$0.92 \leq \mathcal{R}_{0M} < 1$
1	LAS	SFO	SFO
2	SFO	LAS	DEN
3	DEN	DEN	LAS
4	MIA	PHX	LAX

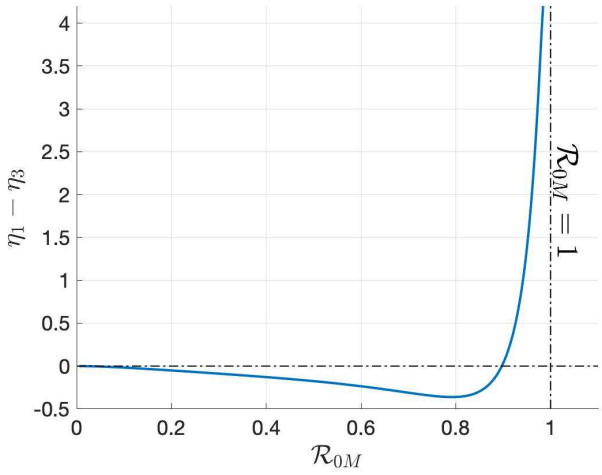

Fig. 3. dynamics-based centrality difference between nodes 1 (Atlanta) and 3 (Chicago) versus network basic reproduction number $\mathcal{R}_{0M}$ for $\tau = 11$ days. The dynamics-based centrality of the two nodes interlace once.

12 days of lag results in approximately 2 percent (which corresponds to a considerable number of individuals in the United States population) increase in the average infection size within 30 days of epidemic onset.

The dynamics-based centrality difference between Atlanta and Chicago with respect to basic reproduction number is shown in Fig. 3. When $\tau = 11$ days, one interlacing between the selected nodes is observed. In other words, as the disease progresses and $\mathcal{R}_{0M}$ increases, Atlanta becomes a more central subpopulation than Chicago, requiring a more restricted traffic control strategy.

Table I presents the top 4 ranking results for different ranges of $\mathcal{R}_{0M}$ when $\tau \to 0$ and $a_{ii} \in [0, 1]$ for all $i \in \mathcal{V}$. As proven by Theorem (2), the output of dynamics-based centrality, $\mathcal{I}_e$, and local centrality, $\mathcal{I}_o$, converge as $\frac{\beta}{\delta} \to 0^+$ or $\mathcal{R}_{0M} \to 0^+$. For the simulated network in particular, when $0 < \mathcal{R}_{0M} < 0.06$, the first 4 central airports based on dynamics-based and local centralities are identical. On the other hand, when $\tau \to 0$, the output of dynamics-based centrality, $\mathcal{I}_e$, will converge to that of eigenvector centrality, $\mathcal{I}_{ev}$, as $\frac{\beta}{\delta} \to \frac{1}{u_n}^-$ or $\mathcal{R}_{0M} \to 1^-$, see Theorem (3). For the studied network, these centralities provide the same top 4 rankings while $0.92 < \mathcal{R}_{0M} < 1$. The simulation results, along with our theoretical findings, indicate that for $\mathcal{R}_{0M} \to 0^+$ and $\mathcal{R}_{0M} \to 1^-$, the effect of epidemic properties on the rankings results is negligible. In such cases, a node's location in the network will be the only factor determining its impact on the network performance. On the other hand, for $0 < \mathcal{R}_{0M} < 1$, the epidemic properties of disease will also contribute to the rankings provided by dynamics-based centrality, which in turn leads to a different output.

Fig. 4(a) presents the transition of dynamics-based rankings in non-delayed network as the reproduction number increases. Since η_i is a nonlinear function of epidemic rates, a non-smooth variation in airport rankings is observed. The initial and final rankings (obtained for $\mathcal{R}_{0M} \to 0^+$ and

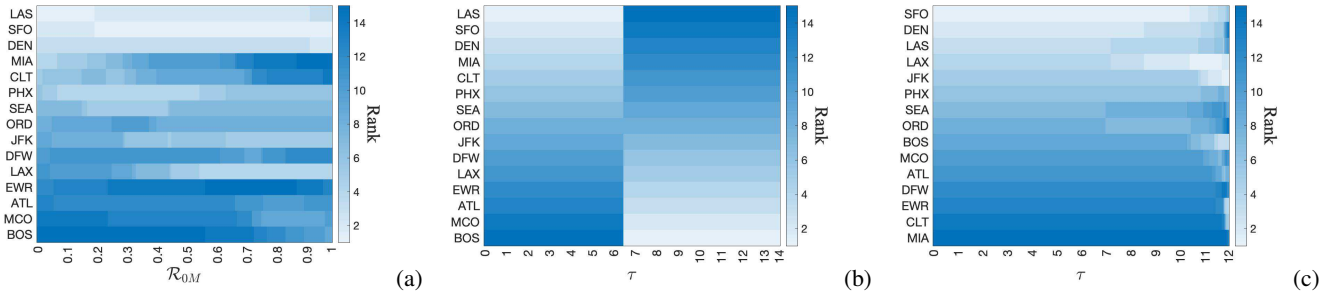

(a) (b) (c)

Fig. 4. Heat map of airport rankings obtained by the dynamics-based centrality with respect to (a) network basic reproduction number $\mathcal{R}_{0M}$ when $\tau \to 0$. (b) time delay τ when $\mathcal{R}_{0M} \to 0^+$. (c) time delay τ when $\mathcal{R}_{0M} \to 1^-$.

$\mathcal{R}_{0M} \to 1^-$, respectively) are equivalent to the rankings found by local and eigenvector centralities, respectively.

The airport rankings provided by dynamics-based centrality for different time delays (in the stable range) when $\mathcal{R}_{0M} \to 0^+$ is shown in Fig. 4(b). As predicted by Theorem 2, when $\tau \approx 6.4$ (equivalent to $\delta\tau = z_1$ in Theorem 2), we observe a sudden shift in the rankings, which reverses the order of central nodes. In this case, the value of internal time delay determines the order of central airports.

Fig. 4(c) shows the dynamics-based rankings for $\mathcal{R}_{0M} \to 1^-$ as time delay increases. An invariant ranking is observed for a certain range of time delay.

VI. Conclusion

The n-intertwined SIS model with internal time delays is studied and a performance measure based on the $\mathcal{H}_2$ norm is developed to evaluate the effect of small shocks, modeled by Gaussian white noise, on the network robustness. This metric is then employed to define a new node centrality index, which evaluates the sensitivity of network performance with respect to shocks to its nodes. Unlike walk-based centralities, such as local or eigenvector centrality, the introduced centrality incorporates the impact of epidemiological properties of the disease to penalize the long closed walks in the network, making it a *dynamics-based* centrality. We prove that for certain choices of parameters, the dynamics-based centrality and resolvent centrality are equivalent. For slightly contagious disease, i.e., significantly low infection rate with respect to recovery rate, we present the correlation between the dynamics-based centrality and two local centralities, one of which turns to degree centrality for the loop-less networks. Moreover, we show that for certain epidemic rates, when internal time delays are negligible, the output of dynamics-based centrality and eigenvector centrality converge. The results obtained in this study are based on certain assumptions, including the use of a linear SIS model and an undirected network. Future research can build upon these findings to explore more complex scenarios.

References

[1] V. Preciado, M. Zargham, C. Enyioha, A. Jadbabaie, and G. J. Pappas, "Optimal resource allocation for network protection: A geometric programming approach," *IEEE Transactions on Control of Network Systems*, pp. 99–108, 2014.

[2] M. Y. Li and J. S. Muldowney, "Global stability for the SEIR model in epidemiology," *Mathematical Biosciences*, vol. 125, no. 2, pp. 155–164, 1995.

[3] A. L. Lloyd and V. A. Jansen, "Spatiotemporal dynamics of epidemics: synchrony in metapopulation models," *Mathematical Biosciences*, pp. 1–16, 2004.

[4] A. Kaddar, A. Abta, and H. T. Alaoui, "A comparison of delayed SIR and SEIR epidemic models," *Nonlinear Analysis: Modelling and Control*, vol. 16, no. 2, pp. 181–190, 2011.

[5] P. Yan and S. Liu, "SEIR epidemic model with delay," *The ANZIAM Journal*, vol. 48, no. 1, pp. 119–134, 2006.

[6] Y. Ding, Z. Jin, and J. Lou, "An SEIS epidemic model on scale-free network with recruitment and death," *Journal of Nonlinear Functional Analysis*, 2015.

[7] M. Siami, S. Bolouki, B. Bamieh, and N. Motee, "Centrality measures in linear consensus networks with structured network uncertainties," *IEEE Transactions on Control of Network Systems*, vol. 5, no. 3, pp. 924–934, 2017.

[8] A. Darabi and M. Siami, "Centrality in epidemic networks with time-delay: A decision-support framework for epidemic containment," in *2021 American Control Conference (ACC)*, pp. 3062–3067, IEEE, 2021.

[9] T. W. Valente, K. Coronges, C. Lakon, and E. Costenbader, "How correlated are network centrality measures?," *Connections (Toronto, Ont.)*, vol. 28, no. 1, p. 16, 2008.

[10] M. Benzi and C. Klymko, "On the limiting behavior of parameter-dependent network centrality measures," *SIAM Journal on Matrix Analysis and Applications*, vol. 36, no. 2, pp. 686–706, 2015.

[11] P. Holme, B. J. Kim, C. N. Yoon, and S. K. Han, "Attack vulnerability of complex networks," *Physical review E*, vol. 65, no. 5, p. 056109, 2002.

[12] F. Chung, P. Horn, and A. Tsiatas, "Distributing antidote using pagerank vectors," *Internet Mathematics*, vol. 6, no. 2, pp. 237–254, 2009.

[13] M. Doostmohammadian, H. R. Rabiee, and U. A. Khan, "Centrality-based epidemic control in complex social networks," *Social Network Analysis and Mining*, vol. 10, no. 1, pp. 1–11, 2020.

[14] A. Darabi and M. Siami, "Robustness analysis of epidemic networks with multiple time-delays," in *2022 American Control Conference (ACC)*, pp. 3668–3674, IEEE, 2022.

[15] C. K. Enyioha, *A convex framework for epidemic control in networks*. University of Pennsylvania, 2014.

[16] Z. Rekasius, "A stability test for systems with delays," in *Joint Automatic Control Conference*, no. 17, p. 39, 1980.

[17] M. Siami and N. Motee, "Fundamental limits and tradeoffs on disturbance propagation in linear dynamical networks," *IEEE Transactions on Automatic Control*, vol. 61, no. 12, pp. 4055–4062, 2016.

[18] Y. Ghaedsharaf, M. Siami, C. Somarakis, and N. Motee, "Eminence in presence of time-delay and structured uncertainties in linear consensus networks," in *2017 IEEE 56th Annual Conference on Decision and Control (CDC)*, pp. 3218–3223, IEEE, 2017.

[19] J. Doyle, K. Glover, P. Khargonekar, and B. Francis, "State-space solutions to standard $\mathcal{H}_2$ and $\mathcal{H}_\infty$ control problems," *IEEE Transactions on Automatic Control*, vol. 34, no. 8, pp. 831–847, 1989.

[20] C. Godsil and J. Smith, "Strongly cospectral vertices," 2017.

[21] T. Opsahl, "The network of airports in the united states." `https://toreopsahl.com/datasets/#usairports`, 2010 (accessed October 26, 2020).